FeelPen

A Haptic Stylus Displaying Multimodal Texture Feels on Touchscreens

Kodak, Bence L.; Vardar, Yasemin

DOI
10.1109/TMECH.2023.3264787

Publication date
2023

Document Version
Final published version

Published in
IEEE/ASME Transactions on Mechatronics

FeelPen: A Haptic Stylus Displaying Multimodal Texture Feels on Touchscreens

Bence L. Kodak and Yasemin Vardar

***Abstract*—The ever-emerging mobile market induced a blooming interest in stylus-based interactions. Most state-of-the-art styluses either provide no haptic feedback or only deliver one type of sensation, such as vibration or skin stretch. Improving these devices with display abilities of a palette of tactile feels can pave the way for rendering realistic surface sensations, resulting in more natural virtual experiences. However, integrating necessary actuators and sensors while keeping the compact form factor of a stylus for comfortable user interactions challenges their design. This situation also limits the scientific knowledge of relevant parameters for rendering compelling artificial textures for stylus-based interactions. To address these challenges, we developed FeelPen, a haptic stylus that can display multimodal texture properties (compliance, roughness, friction, and temperature) on touchscreens. We validated the texture rendering capability of our design by conducting system identification and psychophysical experiments. The experimental results confirmed that FeelPen could render a variety of modalities with wide parameter ranges necessary to create perceptually salient texture feels, making it a one-of-a-kind stylus. Our unique design and experimental results pave the way for new perspectives with stylus-based interactions on future touchscreens.**

***Index Terms*—Electrovibration, haptic interface, haptics, perceptual dimensions, tactile perception, texture rendering.**

I. Introduction

TOUCHSCREENS have gained a vast space in the mobile market as part of computers, tablets, and smartphones. Being able to interact and manipulate digital content—along with engaging visual and auditory cues—provides an intuitive, efficient, and easy usage of touchscreens. Yet, commercially available ones lack vivid haptic feedback that could enable users to touch and feel the digital content; most of them only deliver confirmatory vibrations, such as buzzes and click [1]. Nonetheless, displaying richer tactile sensations could enhance the immersiveness and realism of virtual experiences [2]. When humans touch objects in the physical world, they immediately feel their roughness, softness, friction, and thermal properties; having one or more of these sensations on touchscreens would allow engaging applications. For example, perceiving the fabric of different pieces of clothing while scrolling through an online fashion store or having a simulated pen-on-paper feel while writing on a tablet would enhance the user experience.

One popular approach for providing rich tactile information on touchscreens is using a stylus that can display haptic feedback. These devices allow natural user–computer interaction while eliminating factors that cause contact and perceptual variability in finger–surface interactions [3], [4], [5]. The earlier designs of haptic styluses mainly aimed to improve the user performance and accuracy for precision tasks. These devices guided users by primarily vibrotactile feedback generated by mounted linear resonant actuators [6], pin-arrays [7], vibration motors [8], or piezoelectric actuators [9] within the stylus or on the touchscreen; few provided force feedback on the surface via ballpoint drive [10], [11] or electrostatic actuation [12], [13]. Some designs simulated contact with virtual objects using small dc motors integrated within the stylus [14], [15], [16].

A few haptic styluses focused on emulating material properties, which is the main focus of this article. For example, Romano et al. and Culbertson et al. recorded accelerations between a tool and various surfaces, created texture models, and rendered them via a stylus integrated with a voice-coil actuator [17], [18]. Cho et al. [19] designed a stylus that could provide pen-on-paper feels via a linear resonant actuator by superposing the principal frequencies of real pen–paper interaction. They also enhanced the interaction with simultaneous auditory feedback. Taking inspiration from Wintergerst et al. [20], who used a magnetically operated brake at the stylus tip, Culbertson et al. developed another handheld device that can modulate perceived friction along with roughness using a solenoid and a voice-coil actuator together [21]. Chen et al. proposed a stylus design for displaying object stiffness using force and vibrotactile feedback by integrating three actuators: a piston-type magnetorheological actuator, a voice-coil motor, and a linear resonant actuator [22]. Quek et al. augmented the perceived stiffness by providing skin stretch through the displacement of a tactor under the finger pad [23]. Kruijff et al. modified perceived compliance

Manuscript received 19 October 2022; revised 17 February 2023; accepted 23 March 2023. Date of publication 19 April 2023; date of current version 17 October 2023. This work was supported by the Delft University of Technology. Recommended by Technical Editor M. Indri and Senior Editor Y.-J. Pan. *(Corresponding author: Yasemin Vardar.)*

This work involved human subjects or animals in its research. Approval of all ethical and experimental procedures and protocols was granted by the Human Research Ethics Committee of Delft University of Technology under Application No: 1955, and performed in line with the Helsinki Declaration.

The authors are with the Department of Cognitive Robotics, Faculty of Mechanical, Maritime and Materials Engineering, Delft University of Technology, 2628CD Delft, The Netherlands (e-mail: B.L.Kodak@tudelft.nl; Y.Vardar@tudelft.nl).

This article has supplementary material provided by the authors and color versions of one or more figures available at https://doi.org/10.1109/TMECH.2023.3264787.

Digital Object Identifier 10.1109/TMECH.2023.3264787

by installing a variable-tension flexible layer above the touchscreen [24]. The membrane properties of this layer also allowed simultaneous vibratory cues through an attached speaker while scanning the screen with a stylus.

Unfortunately, the mentioned haptic stylus designs for mobile applications can emulate at most two material properties (roughness and friction or compliance) via the same device, representing only a subset of relevant tactile cues. However, perceptual studies where human participants interacted with physical textures with their bare hands and rated their perceptual properties revealed other perceptually relevant texture properties, such as macro-roughness, compliance, and warmth [25], [26]. The importance of displaying a wide range of tactile cues (hardness, friction, and fine roughness) for realistic texture rendering was also supported by Culbertson et al. by using a force-feedback haptic device (Phantom Omni) integrated with a voice-coil actuator [27]. In this study, roughness cues were conveyed via the voice-coil actuator rendering tool-surface accelerations, while friction cues were via the force-feedback device. For hardness cues, they displayed tapping transients of the surfaces via the Omni device, as LaMotte [28] demonstrated that when interacting with objects via a tool, tapping is a better approach than pressing to perceive their softness. Although this design successfully demonstrated the relevance of displaying different tactile modalities for the realistic rendering of surface feels, it was unsuitable for mobile applications. As styluses need to have a sleek form factor yielding a comfortable user interaction with touchscreens, it is challenging to combine all the necessary sensors and actuators and fit them into the limited space to deliver a wide range of sensations.

This design challenge leads to a knowledge gap of unknown parameter space for salient virtual textures generated via styluses. For example, humans inherently do not feel the thermal properties while interacting with objects via a tool. Therefore, it is unknown whether augmenting this sensation during touchscreen interactions would be a meaningful dimension for virtual texture space. Similarly, the difference between macro- and microroughness may not be crucial, as perception depends on the propagated vibrations from tip–surface interactions [29], [30]. Moreover, it remains unclear whether solely relying on indentation difference while disregarding tapping transients is sufficient for conveying compliance cues with a stylus [28].

To address the aforementioned research questions, we present FeelPen, the first haptic stylus capable of displaying multimodal texture properties (roughness, friction, compliance, and temperature) on touchscreens. We explain our design process in detail and validate the texture rendering capabilities of our device via system identification and psychophysical experiments.

II. Design of FeelPen

The primary design consideration of FeelPen was displaying the feel of a wide range of textural properties, such as surface roughness and friction, thermal characteristics, and compliance, using commercially available sensors and actuators. Moreover, when selecting the components, the balance between size and performance was a decisive aspect, as every piece has to be as small as possible to fit inside a relatively compact pen. The 3-D-printed FeelPen housing consists of four parts connected by a clearance fit for an easier assembly; see Fig. 1 and Supplementary Materials and Video for the overall design of the device and signal workflow between the hardware components. This section explains the working principle, hardware design, and mechanical behavior of FeelPen.

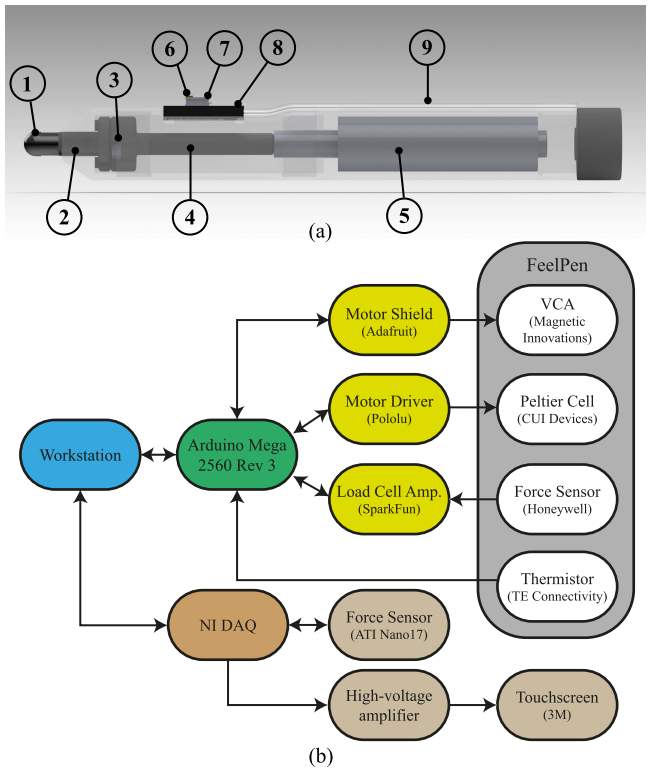

Fig. 1. (a) Design of FeelPen: (1) conductive pen tip, (2) connection rod, (3) load cell, (4) connection rod, (5) voice-coil actuator, (6) thermistor, (7) Peltier cell, (8) water-cooled heat sink, and (9) silicone tubes for water cooling. (b) Signal workflow between the hardware components.

A. Surface Roughness and Friction

FeelPen conveys surface roughness and friction by modulating electrostatic forces generated between a conductive stylus tip and a capacitive touchscreen. When an alternating voltage signal is applied to the conductive layer of the touchscreen, an attractive electrostatic force develops between the insulative layer of the screen and the stylus tip [12]; this force modifies dynamic friction during sliding. This effect, known as electrovibration [31], can produce wide-bandwidth friction forces, have fast dynamics, and require low power [32], [33]. Earlier studies for finger interaction showed that electrovibration is a feasible solution for delivering roughness and friction cues, and texture rendering [34], [35], [36], [37].

In our design, the input voltage signal applied to the touchscreen (SCT3250, 3M Inc.) was first generated by a data acquisition card (PCIe-6323, NI), and then, amplified via a custom-designed amplifier Fig. 2. The stylus tip was electrically grounded to enhance the magnitude of the electrostatic forces [38]. The dc and ac components of the voltage signal

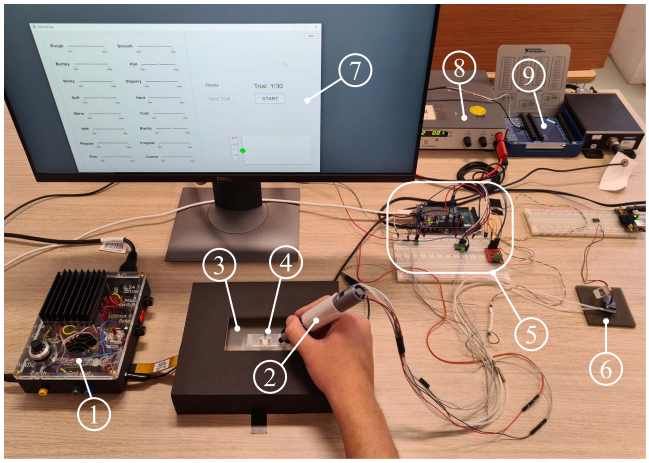

Fig. 2. Experimental setup: (1) amplifier, (2) FeelPen, (3) touchscreen, (4) force sensor, (5) electrical components, (6) miniature water pump, (7) graphical user interface, (8) external power supply, and (9) data acquisition card.

modify the constant and alternating adhesion between the stylus tip and touchscreen, respectively [37]. Hence, by changing the amplitude and frequency components of the input voltage signal, various roughness and friction sensations can be conveyed [39].

Previous studies [4], [40] showed that tactile perception of electrovibration occurs via generated electrovibration force magnitude and frequency, and this force shows a nonlinear dependence on input voltage signal properties, as well as scanning speed and applied pressure. This behavior heavily depends on electromechanical properties of materials at contact—in our case, these are the stylus tip and the touchscreen [41].

Therefore, we identified the range of electrovibration force magnitudes and friction coefficients generated as a function of input voltage while one participant scanned FeelPen on the touchscreen. During the measurements, the first author sat in front of an LCD and the touchscreen attached on top of the ATI Nano17 force sensor Fig. 2. Contact forces were measured by this sensor and sampled by a data acquisition card (PCIe-6323, NI) at 10 kHz.

The input voltage applied to the touchscreen was zero mean sinusoidal signals. Five peak-to-peak amplitudes (40, 80, 120, 160, and 200 V) and ten frequencies, equally spaced on a logarithmic scale from 10 to 1000 Hz (10, 17, 28, 46, 77, 129, 215, 360, 600, and 1000 Hz), were tested. We used the logarithmic scale in which human tactile perception behaves linearly [42]. The first author scanned the display from left to right five times while maintaining 50 mm/s scanning speed and 1 N pressing force; we selected these values as they provided comfortable user interaction demonstrated in our preliminary experiments. The sliding speed was controlled with a metronome, and applied force was shown on LCD via a graphical user interface designed via MATLAB software. Each scan started at a metronome tap and ended at the next one. Contact forces for all combinations of signal amplitude and frequency were recorded ($5 \times 10 = 50$ trials).

To calculate kinetic friction coefficients, first contact forces were low-pass filtered with a cut-off frequency of 1 kHz. Then,

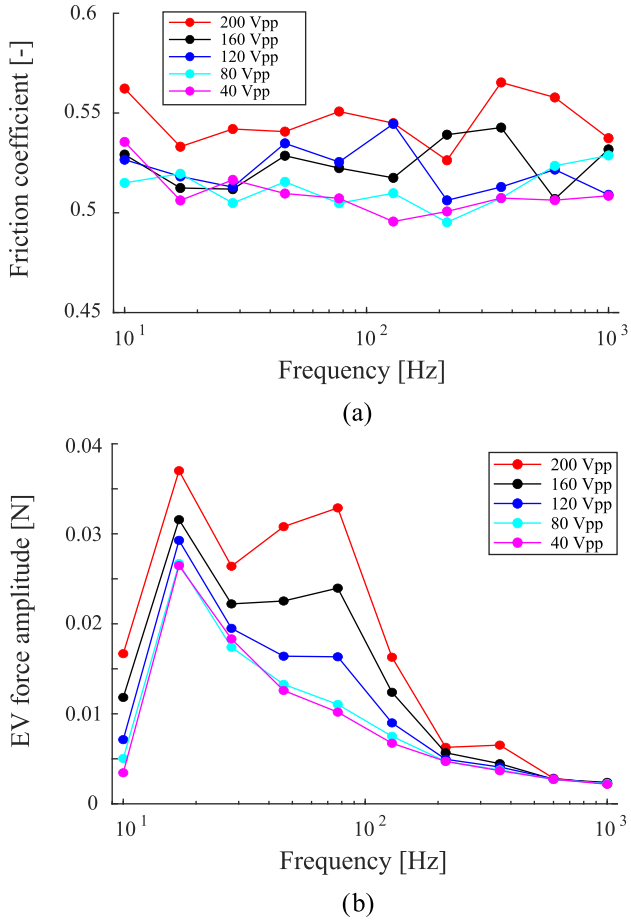

Fig. 3. (a) Friction coefficients and (b) electrovibration force magnitudes measured as a function of voltage signal amplitude.

they were segmented into five pieces, each representing when the sliding was approximately constant. After this, the lateral force segment was divided by the corresponding normal force and averaged to get the coefficient for that segment. The average kinetic friction coefficient for each input voltage frequency–amplitude condition was calculated by averaging the coefficients obtained from the five segments; see Fig. 3(a) for calculated friction coefficients.

When a zero mean sinusoidal voltage signal is applied to the touchscreen, the electrovibration force occurs at twice the input signal frequency [4], [40]. For example, a 10 Hz sinusoidal voltage signal would produce a force oscillating at 20 Hz. The magnitude of the electrovibration forces in both lateral and normal directions was calculated by first filtering the segmented signals via a bandpass filter with the following cutoff frequencies: $2 \cdot f_v \pm 5$ Hz for for voltage signal frequencies (f_v) from 10 to 46 Hz, and $2 \cdot f_v \pm 10$ Hz for f_v from 77 to 1000 Hz. After this, the average power of each filtered signal was calculated. Multiplying the average power by two and taking the square root of this value gave the amplitude of the electrovibration force for each segment. The average electrovibration force magnitude was calculated by averaging over the five segments for each condition and summing the components in lateral and normal directions; see Fig. 3(b) for calculated electrovibration force magnitudes.

TABLE I
PARAMETERS OF THE VOICE-COIL ACTUATOR

Coil resistance [Ω]	11.3 ± 0.5
Coil inductance [mH]	1.93 ± 0.2
Force sensitivity, middle pos. [N/A]	$2.6 \pm 8\%$
BEMF constant, middle pos. [Vs/m]	$2.6 \pm 8\%$
Moving magnet mass [g]	$17.9 \pm 8\%$
Stroke length (in one direction) [mm]	9
$K_{\mathrm{F}}(x)$ [N/A]	$-0.01x^2 - 0.00021x + 2.58$

B. Material Compliance

When using a tool for compliance perception, the primary cues are kinesthetic due to the absence of direct skin contact with the material [43]. Users mostly perceive material compliance by tapping or indenting on the surface with a tool [28]. In the first case, the main determining factors of compliance are the frequency components of the generated tapping transients, whereas for the latter, the ratio of the indentation depth of the tool to the exerted force.

FeelPen exploits this latter case of our compliance perception. Users act against various force levels as they indent the FeelPen on the touchscreen—this feel is similar to pushing against springs with different stiffness values. These forces are rendered with a commercially available voice-coil actuator, which provides a wide force range within a compact form with a fast response [44]. For our design, we required an actuator with an outer diameter of 16 mm or smaller, having a stroke length of at least 6 mm, and the capability of providing at least 2 N maximum continuous force. Given these requirements, we chose the voice-coil actuator MI-MMB 1555 (Magnetic Innovations Inc.). The parameters of the voice-coil actuator can be found in Table I.

When FeelPen is indented, the user's force from the stylus tip is transmitted through a rod connecting to the voice-coil actuator's moving magnet with a threaded shank. The entire mechanism moves together inside the stylus; the base of this movement is the outer shell of the voice-coil placed stably inside the housing. The force generated by a voice-coil actuator depends on the position of the moving magnet and is maximum when the moving magnet is in the middle position inside the stator. Hence, we designed the inner mechanism such that the maximum force is present when the pen is fully indented; this is when the moving magnet reaches the middle position. The stroke force of the actuator is modified proportionally to the compliance of the emulated material. So, when one pushes down the FeelPen, they can feel various force levels as a function of indentation, counteracting the force generated by the actuator. The voltage input signal sent to the voice-coil actuator is amplified by a motor driver (Motor Shield v2.3, Adafruit Inc.) to supply the necessary power. The user's pressing force can also be measured with a force sensor (060-2443-06, Honeywell International Inc.), and the voltage data read by the sensor is sent to a microcontroller (Mega 2560 Rev 3, Arduino Inc.) through a load cell amplifier (HX711, SparkFun Electronics).

Identifying the force characteristics of the voice-coil actuator is an essential step for emulating material compliance. Hence, we modeled the electrodynamic behavior of the voice-coil actuator and validated it with measurements. As the voice-coil actuator operated for relatively short time periods in our application, the thermal effects were neglected. The force generated by the voice-coil actuator is acting based on the Lorentz principle

$$F_{\mathrm{VCA}} = K_{\mathrm{F}}(x) \cdot I \tag{1}$$

where $K_{\mathrm{F}}(x)$ is the force sensitivity of the actuator and I is the current flowing through the coil. $K_{\mathrm{F}}(x)$ is dependent on the position of the moving magnet along the cylinder axis. Using a voltage-drive circuit, the actuator current I is indirectly controlled based on the electromechanical dynamics of the actuator

$$E = RI + K_{\mathrm{B}}\frac{dx}{dt} + L\frac{dI}{dt} \tag{2}$$

where E is the voltage sent to the actuator, R is the wire resistance, L is the coil inductance, $K_{\mathrm{B}} \cdot dx/dt$ is the back-electromotive force (BEMF) induced by the moving magnet inside the coil, and K_{B} is the BEMF constant. The dynamic model of the voice-coil actuator can be driven by applying Newton's second law to the moving magnet of the actuator, using (1) and (2). When the mass of the moving cylinder is m and the external load on the cylinder is F_{ext}, the dynamic model is the following:

$$F_{\mathrm{VCA}} - F_{\mathrm{ext}} = m\frac{d^2x}{dt^2}. \tag{3}$$

This model is limited to considering motion along one axis only. The extent of the off-axis movement is influenced by the hand grip configuration, which was not assessed in the study. To minimize significant off-axis motion, participants were instructed to hold the pen perpendicular to the screen.

We validated our Simulink model via laboratory experiments. The test bed consisted of a force sensor (Nano17, ATI Inc.) and an adjustable frame where the pen can be placed stably in a horizontal position. Force characteristics of the voice-coil actuator were tested with a ramp voltage signal (slope 3.9 V/s, $V_{\mathrm{max}} = 10\,V$) for four different positions of the moving magnet. These were the middle position of the magnet inside the stator, and 2, 5, and 8 mm from the middle of the stator. The voltage signals were sent to the actuator from the microcontroller at 100 Hz and the forces were sampled by a data acquisition card (PCIe-6323, NI) at 1 kHz. Five different measurements were taken for each magnet position.

The simulated and measured force characteristics of the actuator are shown in Fig. 4. The mean absolute error values between simulated and measured forces are: 0.054, 0.093, 0.057, and 0.03 N for the middle, 2, 5, and 8 mm positions, respectively. The validated model allows us to simulate the force values of the actuator as a function of the indentation depth of the pen for different constant input voltages sent to the actuator Fig. 5. The black line marks the maximum forces available with the device.

C. Material Thermal Properties

FeelPen provides thermal cues by a Peltier cell (CP076581-238, CUI Devices) placed at the finger grip location on the

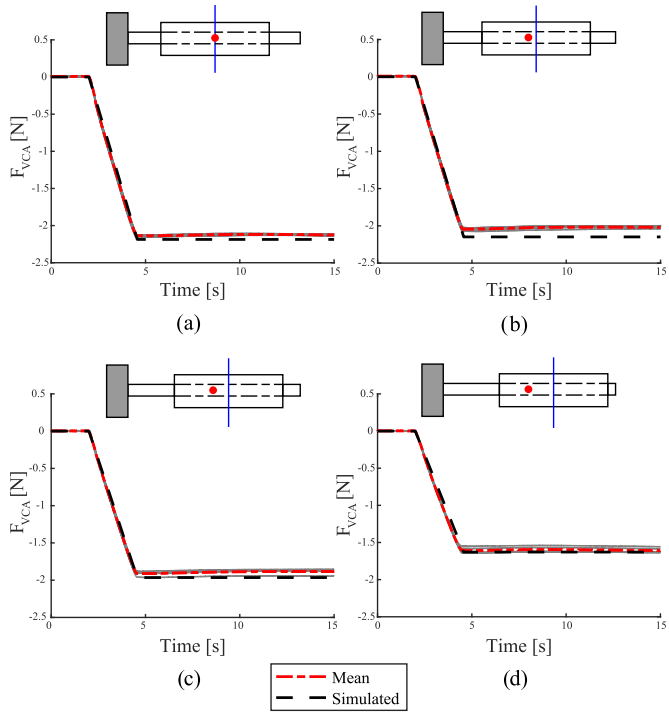

Fig. 4. Simulated and measured force characteristics of the voice-coil actuator. (a) Magnet in the middle position. (b)–(d) Magnet moved 2, 5, 8 mm from the middle position, respectively. The blue vertical lines and the red dots represent the middle of the stator and the middle of the moving magnet, respectively; the gray rectangles represent the force sensor of the test bed. The gray lines represent the individual force measurements, whereas the red dashed lines indicate their mean. The black dashed lines show the simulated forces.

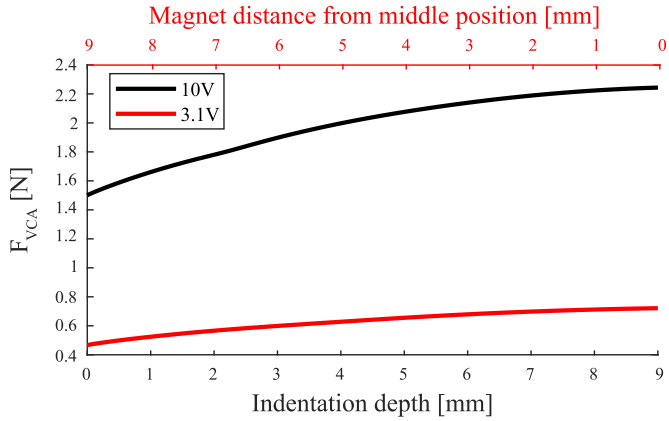

Fig. 5. Generated force versus indentation depth behavior of the voice-coil actuator for constant voltages. The moving magnet is in the middle position at 9-mm indentation depth of the pen.

housing, which is driven by a compact H-bridge motor driver board (DRV8835, Pololu Corporation) powered by an external power supply (ES 030-50, Delta Elektronika). We selected this Peltier cell model based on its small geometry and heat flux generation capability. It can easily fit under the area of the user's index finger while holding the pen and create the required heat flux for fast, accurate, and distinguishable thermal cues.

A miniature, water-cooled aluminum heat sink (overall dimensions 22x12x4 mm) was designed to dissipate the heat pumped by the Peltier cell, similar to [45]. A compact water pump (480-188, RS PRO) circulates the water inside the heat sink. The heat sink and the water pump are connected with flexible silicone tubes (1030S0003414, Technirub International BV). Finally, a miniature thermistor (GA10K3MCD1, TE Connectivity) is placed on top of the Peltier cell. As the user's index finger covers both the thermistor and the Peltier cell, we can directly control the Peltier-finger contact temperature by the Arduino microcontroller.

The sensing range of human thermoreceptors is between 5 °C and 45 °C; sensation of pain occurs when the temperature falls below 15–18 °C or rises above 45 °C [46]. As the resting temperature of the skin is usually higher than the ambient temperature, the perceived thermal property of materials is related to the rate of heat extraction from the fingers. The rate of temperature change also plays a role, as the initial rapid temperature change seems to invoke the strongest sensations when touching a material [47]. So, all these factors should be considered for emulating the feel of thermally differentiable materials.

The goal of the thermal module is to obtain stable and accurate temperature feedback in the painless temperature range (15–40 °C). The thermal module was controlled by a PID algorithm with feed-forward control. Preliminary tests on the thermal module revealed an asymmetric system behavior, which led to the implementation of two sets of PID controller parameters, one for heating up the finger pad and one for cooling it down. The temperature control algorithm was computed on the microcontroller with a sampling frequency of 100 Hz. The characterization of the thermal module included two experimental sessions, each performed in a laboratory with an ambient room temperature of 20 °C.

The first experiment evaluated the temperature-tracking performance and stability of the thermal module while the finger was in constant contact with the device. The initial contact temperature was set to 28 °C, and step signals with four different reference temperatures (15 °C, 22 °C, 34 °C, and 40 °C) were chosen to evaluate both the cooling and heating performance of the module. Five measurements were conducted for each of the reference temperatures. See the average step response curves of the first experiment in Fig. 6.

The second experiment evaluated the temperature response of the module at the initial finger contact. With this, we calculated the time needed to reach a reference temperature once someone touches the module. The experimenter touched the Peltier cell, while a set of constant reference temperatures (15 °C, 22 °C, 28 °C, 34 °C, and 40 °C) were tracked. Five measurements were conducted for each of the reference temperatures. For the cooling phase, the highest mean settling time was 2.55 s for the reference temperature of 15 °C, whereas, for the heating phase, the highest mean settling time was 3.93 s for the reference temperature of 34 °C.

III. Psychophysical Experiment

In the previous section, we showed that FeelPen has a parameter space covering different modalities relevant to texture perception. However, this information does not directly imply that the users pertinently perceive the textures generated within this

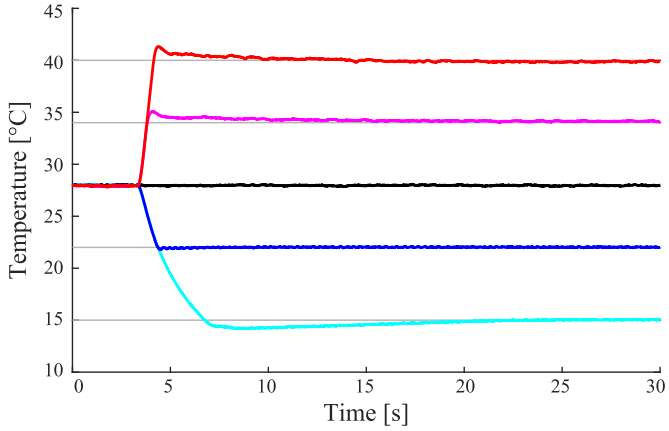

Fig. 6. Step response curves of the closed-loop system for four reference temperatures. The gray lines represent the reference temperatures.

parameter space. Therefore, we also conducted a psychophysical experiment to identify the capability of the FeelPen to create salient texture sensations. The participant's task was to explore various artificial textures generated with the device and rate them on a set of adjective scales.

A. Participants

Six women and 14 men with an average age of 25.1 years (standard deviation, SD: 2.39) participated in the psychophysical experiment. Only two participants were left-handed, and none of the subjects had previous or current visual or sensory-motor disabilities. The experimental procedures were approved by the Human Research Ethics Committee at the TU Delft (approval number 1955). All participants gave informed consent.

B. Experimental Setup

In the experiments, the apparatus described at Section II was used Fig. 2. The touchscreen was covered by a cardboard case with a 9×5 cm rectangular cutout. An elastic adhesive bandage was put on the middle part of the pen to avoid additional thermal stimuli on the thenar webspace from the possible heating of the voice-coil motor. Participants wore noise-cancellation headphones (QC35 II, Bose) with pink noise to mask any auditory cues. The LCD was used for interacting with a graphical user interface. Participants gave their responses with a computer mouse.

C. Stimuli

The perceptual evaluation was addressed by creating a virtual texture design space with distinguishable features. One of the advantages of using artificial textures is that we can choose and adjust their physical parameters. However, it is not so clear, which are the best parameters for synthesizing distinguishable texture properties. Friesen et al. chose amplitude, frequency, and irregularity of sinusoidal voltage signals as the perceptually relevant features on an electrovibration display for fingertip interactions, where irregularity refers to the width of the spectral content around the center frequency [37]. We were inspired by this approach and expanded it with temperature and the stroke force of the voice-coil actuator in order to enhance the multimodality of the device and possibly capture the entire perceptual space of the four major tactile dimensions.

Based on the measured electrovibration force magnitudes Fig. 3, we chose amplitude (120 and 200 Vpp) and center frequency (17, 77, and 360 Hz) values that induced distinct magnitudes and thus easily perceived differences.

Following [37], the voltage signals were constructed from white noise that was made uniform in the [-1,+1] range. This white noise was filtered with the following filter:

$$H(z) = \frac{\frac{\sin w_0}{2Q} - \frac{\sin w_0}{2Q} z^{-2}}{\left(1 + \frac{\sin w_0}{2Q}\right) - (2\cos w_0)\, z^{-1} + \left(1 - \frac{\sin w_0}{2Q}\right) z^{-2}} \tag{4}$$

where the Q-factor and w_0 are calculated as

$$Q = \frac{1}{R} \tag{5}$$

$$w_0 = \frac{2\pi f_0}{f_s}. \tag{6}$$

In (5) and (6), R is the irregularity value, f_0 is the center frequency of the sinusoidal signal, and f_s is the sampling frequency (10 kHz). The lower the value of the irregularity, the more the signal resembles to a simple sine wave. After filtering, the signals were divided by their upper envelopes to get a maximum amplitude of one in the time domain. The amplitude of the signal was changed by scaling. For the experiment, we selected R values of 0.0001, 0.34, and 1.67, as these values provided salient stimuli based on our preliminary observations with four participants.

For displaying material compliance, we selected two constant voltage levels as the input to the voice-coil actuator (3.1 and 10 V, see Fig. 5). Initially, the pen tip was at its maximum stroke length in both cases. When the user indented (pressed) the pen on a "more stiff" artificial material, the higher voltage value was sent to the actuator, consequently exerting a higher force on the skin for the same indentation (pressure). As the main factor for softness discrimination with a tool is the ratio of the indentation depth of the tooltip to the exerted force, this principle enabled us to provide two different compliance sensations.

When delivering thermal cues to the hand, the resting skin temperature is of great importance, as the difference in skin temperature between individuals can cause each person to perceive the thermal cues on a display differently. The constant contact between the thermal module and the index finger of the participants enabled us to set the resting skin temperature to 28 °C for each individual before each trial. From this level, at the beginning of each trial, the index finger was either cooled down to 22 °C, warmed up to 40 °C or remained at the same temperature level. Step signals were used as reference temperatures, similar to those in the characterization experiments Fig. 6. For the experiments, we used the 22 °C to 40 °C temperature range because we found the temperature levels below 22 °C were felt uncomfortable, some even painful, by conducting a pilot study

TABLE II
PARAMETER VALUES OF THE DESIGN WORKSPACE

Center frequency [Hz]	17, 77, 360
Amplitude [Vpp]	120, 200
Irregularity [-]	0.0001, 0.34, 1.67
Temperature levels [°C]	22, 28, 40
Voltage on VCA [V]	3.1, 10

with four participants. Therefore, we set the cold temperature limit there, potentially staying in a comfortable region for most participants.

Table II summarizes all the selected parameter values. The combination of the parameters ($3\times2\times3\times3\times2$) yielded 108 different textures. However, in order to avoid fatigue among participants, we had to reduce the duration of the experiment, so we kept only those parameter combinations that were perceptually distinct from the others. As a result, we tested 60 textures in total. The stimuli set and the detailed selection criteria can be found in the Supplementary Materials.

D. Adjectives

A set of sensory adjectives was composed of the touch lexicon proposed in [48] and the adjective list in [49]. Based on preliminary tests, only 16 sensory adjectives were chosen: rough, smooth, bumpy, flat, sticky, slippery, soft, hard, warm, cold, stiff, elastic, regular, irregular, fine, and coarse.

E. Experimental Procedure

Participants were asked to execute two exploratory patterns (pressure and lateral motion) while holding FeelPen in their dominant hand and interacting with a graphical user interface (GUI). The experiment consisted of three sessions, and the following tasks had to be performed in each session.

Each participant sat in front of the experimental setup. At the beginning of each trial, they pressed the start button and heard a sound cue indicating the start. After this, they pressed the pen three times on the leftmost part of the cutout of the screen while trying to reach the 1.5 N pressing force (marked with a red ball) by following a virtual force gauge indicated on the GUI. They were also asked to hold the device perpendicular to the screen while pressing. After the third press, they stayed at the 1 N level indicated by the force gauge. Then, after another sound cue, the red ball turned green on the GUI and started moving back and forth with a constant speed of 50 mm/s. The task was to follow this green ball while sliding on the screen with the pen and maintaining an applied force at around 1 N. The ball went back and forth twice from left to right. The end of the trial was indicated by another sound cue. Afterward, participants rated the textures based on 16 adjectives by moving sliders for each adjective. Once they were ready, they could proceed with the next trial. Each trial could be played a maximum of two times, and there were no time constraints on the duration of ratings. Readers can refer to Supplementary Video for the experimental procedure.

The first session was a training session with ten trials, giving the participants ten noticeably distinct stimuli. This session helped them become comfortable with the experimental setup and the procedure, as well as ensured that they were acquainted with a wide range of textures. Participants were asked to rate the textures in the next two sessions based on the stimuli of this training session. Their ratings in the training session were not recorded.

The 60 stimuli were divided into two sets of 30 trials in two consecutive sessions with a 5–10 min break in between. The order of stimuli was randomized in both sessions. Participants rated each texture on each sensory adjective scale. The scales were dimensionless, and their two ends were labeled as max and min. Participants gave their answers based on how strongly the given adjective described the given texture. The duration of each 30-trial session was about 30–45 min, and the entire experiment lasted around 1.5–2 h. The $60 \times 16 = 960$ sensory adjective ratings from each participant were the primary data for analysis.

IV. RESULTS

The adjective ratings were normalized by calculating z-scores of each adjective scale within participants. The normalized adjective ratings were then averaged across all participants, resulting in a 60×16 matrix (number of stimuli $\times$ number of adjectives). This matrix was analyzed by a principal component analysis (PCA). For that, we first verified whether the data was applicable for PCA using Bartlett's test of sphericity and the Keyser–Meyer–Olkin (KMO) criterion. Barlett's sphericity test checks whether the null hypothesis of the correlation matrix is an identity matrix; if this hypothesis is rejected, variables can be analyzed by PCA. In our case, Bartlett's test of sphericity was significant, $\chi^2 = 1739.47, p < 0.001$, so there were meaningful correlations across adjectives. The KMO criterion measures sampling adequacy indicating the proportion of variance in the variables caused by underlying factors. KMO score takes values between 0 and 1, and the higher the KMO score, the more suited the data is to PCA. For our data, the KMO score was found as 0.759, indicating "middling" suitability for PCA. Based on Kaiser's criterion, we extracted four principal components, which explained 93.64% of the total variance.

After extracting the principle components, we applied varimax rotation on the component matrix [50]. The goal of the rotation was to improve the interpretability of the component matrix by reaching a simple structure (see Table III for the rotated component matrix with the four components and their corresponding loadings). The biplot in Fig. 7 projects the individual observations and the loadings for the first two components. Each component is described through the adjectives using the following criteria:

1) the absolute value of the component loading is >0.75 for the adjective and
2) the loading is higher on that component than on any other component (see the highlighted component values in Table III).

After conducting PCA, we calculated Pearson correlation coefficients between the parameters of the texture design space

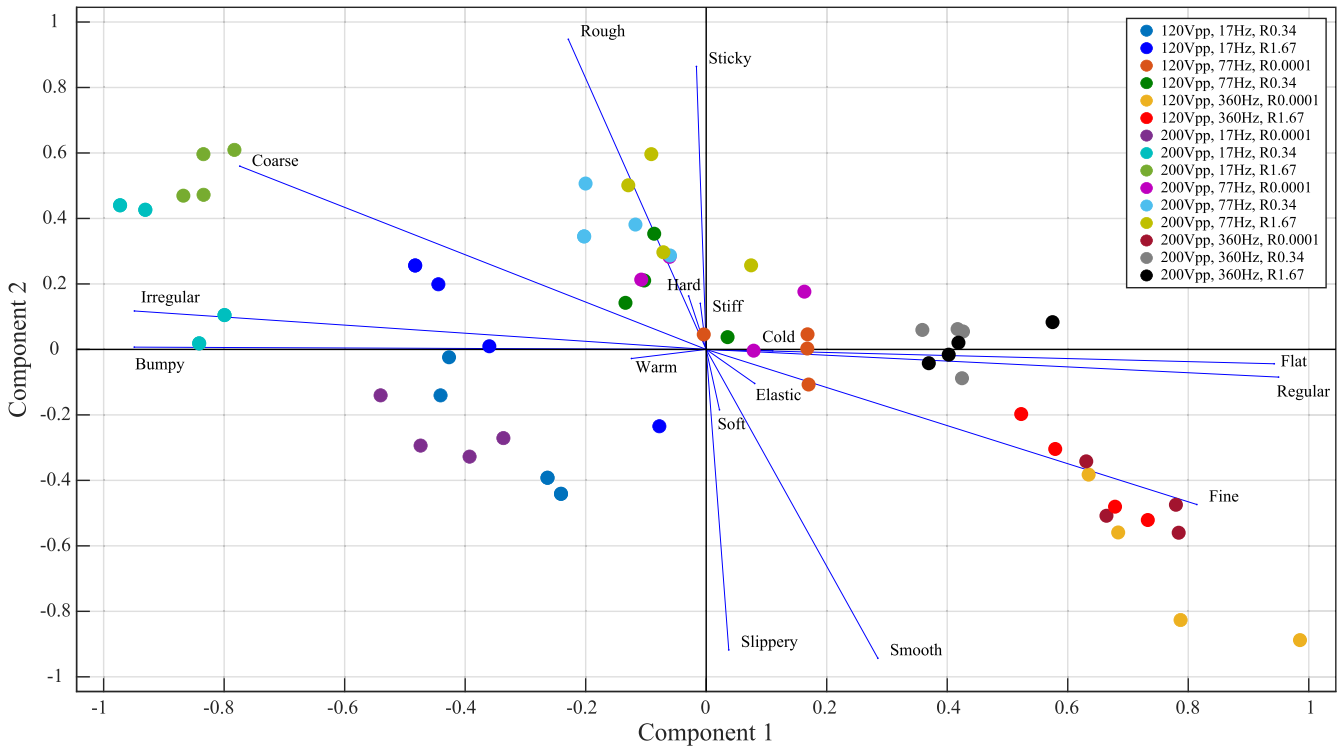

Fig. 7. Visualization of component loadings and scores of the first two components. The observations are color-coded, where each color represents four stimuli with the same touchscreen voltage amplitude, frequency, and irregularity values. The points with the same color have different thermal and compliance properties, but these are not indicated here, as their loadings on the first two components are negligible.

TABLE III
ROTATED COMPONENT MATRIX

Adjectives	Components			
	1	2	3	4
Rough	-0.242	0.928	0.080	0.012
Smooth	0.296	-0.929	-0.039	0.022
Bumpy	-0.935	0.024	0.012	0.121
Flat	0.930	-0.057	-0.029	-0.144
Sticky	-0.007	0.904	0.267	-0.031
Slippery	0.035	-0.942	-0.233	0.016
Soft	0.022	-0.187	-0.960	-0.038
Hard	-0.033	0.157	0.972	0.028
Warm	-0.128	-0.035	0.013	0.982
Cold	0.110	-0.005	0.012	-0.985
Stiff	-0.010	0.141	0.970	0.007
Elastic	0.083	-0.099	-0.951	0.065
Regular	0.959	-0.062	0.024	0.002
Irregular	-0.957	0.097	0.005	-0.006
Fine	0.825	-0.459	-0.137	-0.097
Coarse	-0.787	0.543	0.144	0.111

and the standardized adjective ratings to see how each parameter affects the ratings of different adjectives. Fig. 8 shows the correlation coefficients between the texture parameters and the sensory adjective ratings.

V. DISCUSSION

This study presents FeelPen, a one-of-a-kind haptic stylus capable of conveying multimodal texture properties on touchscreens. We conducted identification experiments to understand the dynamic behavior of the device and psychophysical experiments to test the rendering capability of FeelPen.

A. Texture Rendering Capabilities of FeelPen

Identification experiments showed that FeelPen could successfully display surface friction, roughness, compliance, and thermal properties, although some modalities have a more significant range than others. For example, the friction coefficient can only be modulated by 10% [compare red and pink lines in Fig. 3(a)], on the other hand, compliance can have values with up to 30% difference (check stroke force behavior in Fig. 5). The generated electrostatic forces with the stylus can go up to 0.04 N between 10–1 k Hz with 1-N pressing force [see Fig. 3(b)]. Our results show that this magnitude was sufficient to create different surface roughness by tuning input voltage amplitude, central frequency, and spectral width. Finally, the thermal module can set finger contact temperatures from 15 to 40 °C with a sufficiently fast response Fig. 6.

Psychophysical experiments proved that these parameter ranges enable FeelPen to generate perceptually salient artificial textures; the PCA analysis demonstrated that the created artificial textures by FeelPen can induce—for the first time on a touchscreen—perception in four psychophysical dimensions (see Table III). Here, the first rotated component explains 31.6% of the total variance, and it is described by adjectives "bumpy," "flat," "regular," "irregular," "fine," and "coarse"; see Fig. 7. These adjectives seem to carry macroscopic texture properties similar to gratings in natural materials. Therefore,

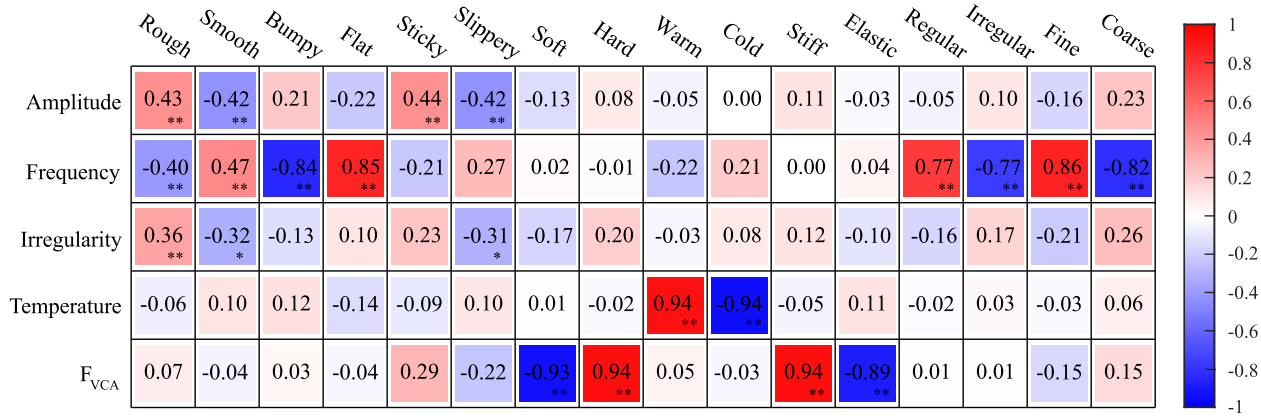

Fig. 8. Correlation matrix, showing the correlations between sensory adjectives and the five texture parameters. The Pearson correlation coefficients between -1 and +1 are color coded (see the color bar on the right). The significance values are marked as ** $p < 0.01$ and * $p < 0.05$.

this component could be interpreted as the virtual equivalent of macroscopic roughness. The second rotated component explains 25.3% of the total variance, and it is described by "rough," "smooth," "sticky," and "slippery" adjectives. There is also a moderate loading on "fine" and "coarse" adjectives. This component seems to associate with the combination of microscopic roughness and friction dimensions. The third rotated component explains 24.3% of the total variance and is defined by "soft," "hard," "stiff," and "elastic" adjectives. This component seems to link to the softness/hardness material property. The fourth rotated component explains 12.5% of the total variance and is described by "warm" and "cold" adjectives. This component relates to the perceptual dimension of coldness/warmth.

With the capability of inducing sensations in four perceptual dimensions with an artificial texture set composed of five parameters, FeelPen outperforms the existing haptic devices in terms of variation of generated texture sensations. For example, earlier studies conducted with tool-based devices [51], [52] revealed a 2-D perceptual space, whereas three studies conducted on electrovibration displays via bare-finger interactions revealed a 3-D perceptual space [37], [53]. Surprisingly, we found two dimensions related to electrovibration despite having the same three parameters as Friesen et al. [37]. The discrepancy could be caused by differences in their experimental approach, including three amplitude values, finger-based interaction, and the application of multidimensional scaling for dimension extraction. Comparing our work to Mun et al., differences may stem from the selected number of parameters (five versus three) and adjectives for texture rating [53]. Nonetheless, with the ability to generate compliance and thermal cues in addition to roughness and friction, FeelPen could generate the widest gamut of tactile textures among the available haptic devices.

B. Relation of Design Parameters to Perceptual Dimensions

The correlation results Fig. 8 revealed that touchscreen voltage frequency, Peltier temperature, and the VCA force are the most relevant parameters for the retrieved perceptual dimensions. On the other hand, amplitude and irregularity showed moderate correlations with the selected adjectives.

The voltage signal frequency was moderately correlated with smoothness and (negatively) roughness. However, it was highly related to flatness, regularity, and fineness, and there was a high negative correlation with bumpiness, irregularity, and coarseness. Frequency seems to be a salient texture parameter in stylus-based interactions.

The amplitude of the voltage signal correlates best with rough, smooth, sticky, and slippery adjectives. This seems plausible, as a higher voltage amplitude implies greater electrostatic adhesion, thus higher frictional forces between the stylus tip and the touchscreen.

There was only a moderate correlation between irregularity and rough/smooth adjectives. The high correlation between frequency and the regular/irregular adjectives indicates that the irregularity parameter alone does not sufficiently alter our perception of texture regularity.

The exerted force of the voice coil actuator correlated highly with hardness and stiffness, and there is a high negative correlation with softness and elasticity. This behavior shows that applying different stroke force levels via the voice-coil actuator can simulate texture sensations with various softness. This finding supports the earlier studies that claimed the softness of objects could be discriminated while actively pressing on them via a stylus [28], [43].

The results showed strong correlations between the temperature of the thermal module, and coldness and warmth sensations. This finding indicates that applying step reference signals to the thermal module provided sufficient fast temperature changes on the finger to generate thermally differentiable material feels. Supporting these findings, in an early study, Yamamoto et al. showed that a rapid temperature change in the early sensation phase plays a crucial role in material recognition by invoking a stronger sensation [47].

C. Comparison to Previous Haptic Styluses

To place FeelPen on the palette of haptic styluses, we compared its performance range for each modality with the ones in the literature. For friction, the stylus of Culbertson et al. was capable of rendering friction coefficients between 0.2 and 0.52, however, for higher values ($\mu \geq 0.35$), the normal force should

be restricted to avoid overheating [21]. FeelPen can also generate friction coefficients up to 0.55 for normal forces of 1 N; the overall range would highly depend on the applied normal force and scanning speed. To the best of our knowledge, no earlier study has measured the electrovibration force magnitudes with a stylus, so it was not possible to compare its performance to earlier work. For compliance, the MH-Pen of Chen et al. was able to provide an output force of 17 N [22]. Although FeelPen cannot reach this force value, its range is sufficient to provide distinct compliance cues. The thermal performance of FeelPen is comparable to previous thermal module designs [45], [54] that gave the inspiration to place a miniature thermal module on the FeelPen. Therefore, we can conclude that FeelPen can render a variety of modalities with wide parameter ranges necessary to create perceptually distinct augmented texture feels, making it a one-of-a-kind stylus.

D. Limitations, Future Work, and Potential Applications

This study had several limitations that could be addressed in future studies. For example, due to the time constraints of the psychophysical experiments, the number of texture parameters was kept minimal; a richer stimuli range could have revealed even more perceptual dimensions. Moreover, the results obtained via the semantic differential method are inherently limited to the selected adjectives [25]. Also, the unequal modulation ranges for rendering parameters could have affected the resulting perceptual dimensions. Moreover, in this work, the participants interacted with FeelPen by holding it perpendicular to the touchscreen. Although the mechanism works with a usual pen grasp (with some leaning), we instructed participants to interact that way as the leaning angle of the pen could affect the indentation depth of the voice-coil actuator, changing the identified parameter space.

In the future, it is also possible to collect data from natural textures and render them via FeelPen. In that case, texture models governing the relation between the input parameters of FeelPen (input voltage to touchscreen, VCA, and Peltier) and texture features are required. However, representing natural textures with only a few parameters is challenging. Nonetheless, several studies [55], [56], [57] seek solutions for that. Suggested features include physical roughness, vibratory power, slide spectral centroid for rough-smooth, compressibility, compliance, tap spectral centroid for hard-soft, and friction coefficient for sticky-slippery dimensions. As the perceived realism of rendered textures also depends on the user exploration speed [27], a position sensor would need to be integrated into the system.

In conclusion, FeelPen is a unique haptic interface capable of creating a wide variety of texture feels on touchscreens. Potential applications of the FeelPen may include immersive gaming experiences on mobile devices, the augmented surface feels during online shopping, and others for entertainment and educational purposes. Another exciting application could be graphical design software for painting, where FeelPen could deliver textural cues of different brushes and pencils, and also mimic the softness and thermal properties of these painting tools, providing a more natural interaction between the human and computer.

Acknowledgment

The authors would like to thank A. Hunt and R. F. Friesen for their insights and fruitful discussions on the device design and rendering processes, respectively. The authors would also like to thank B. Javot and K. J. Kuchenbecker for lending their high-voltage amplifier.

References

[1] M. Fukumoto and T. Sugimura, "Active click: Tactile feedback for touch panels," in *Proc. Extended Abstr. Hum. Factors Comput. Syst.*, 2001, pp. 121–122.
[2] H. Culbertson, S. B. Schorr, and A. M. Okamura, "Haptics: The present and future of artificial touch sensation," *Annu. Rev. Control, Robot., Auton. Syst.*, vol. 1, no. 1, pp. 385–409, 2018.
[3] S. M. Pasumarty, S. A. Johnson, S. A. Watson, and M. J. Adams, "Friction of the human finger pad: Influence of moisture, occlusion and velocity," *Tribol. Lett.*, vol. 44, no. 2, pp. 117–137, 2011.
[4] Y. Vardar and K. J. Kuchenbecker, "Finger motion and contact by a second finger influence the tactile perception of electrovibration," *J. Roy. Soc. Interface*, vol. 18, no. 176, 2021, Art. no. 20200783.
[5] G. Serhat, Y. Vardar, and K. J. Kuchenbecker, "Contact evolution of dry and hydrated fingertips at initial touch," *PLoS One*, vol. 17, no. 7, 2022, Art. no. e0269722.
[6] K.-U. Kyung, J.-Y. Lee, J. Park, and M.A. Srinivasan, "Wubi-pen: Sensory feedback stylus interacting with graphical user interface," *Presence, Teleoperators Virtual Environ.*, vol. 21, no. 2, pp. 142–155, 2012.
[7] K.-U. Kyung and J.-Y. Lee, "Ubi-pen: A haptic interface with texture and vibrotactile display," *IEEE Comput. Graph. Appl.*, vol. 29, no. 1, pp. 56–64, Jan./Feb. 2009.
[8] A. Arasan, C. Basdogan, and T. M. Sezgin, "Haptistylus: A novel stylus for conveying movement and rotational torque effects," *IEEE Comput. Graph. Appl.*, vol. 36, no. 1, pp. 30–41, Jan./Feb. 2016.
[9] I. Poupyrev, M. Okabe, and S. Maruyama, "Haptic feedback for pen computing: Directions and strategies," in *Proc. Extended Abstr. Hum. Factors Comput. Syst.*, 2004, pp. 1309–1312.
[10] S. Kianzad and K. E. MacLean, "Harold's purple crayon rendered in haptics: Large-stroke, handheld ballpoint force feedback," in *Proc. IEEE Haptics Symp.*, 2018, pp. 106–111.
[11] S. Kianzad and K. E. MacLean, "Collaborating through magic pens: Grounded forces in large, overlappable workspaces," in *Proc. Int. AsiaHaptics Conf.*, 2018, pp. 233–237.
[12] Q. Wang, X. Ren, S. Sarcar, and X. Sun, "EV-Pen: Leveraging electrovibration haptic feedback in pen interaction," in *Proc. ACM Int. Conf. Interactive Surf. Spaces*, 2016, pp. 57–66.
[13] Q. Wang, X. Ren, and X. Sun, "Enhancing pen-based interaction using electrovibration and vibration haptic feedback," in *Proc. CHI Conf. Hum. Factors Comput. Syst.*, 2017, pp. 3746–3750.
[14] S. Kamuro, K. Minamizawa, N. Kawakami, and S. Tachi, "Ungrounded kinesthetic pen for haptic interaction with virtual environments," in *Proc. IEEE 18th Int. Symp. Robot Hum. Interactive Commun.*, 2009, pp. 436–441.
[15] A. Withana, M. Kondo, Y. Makino, G. Kakehi, M. Sugimoto, and M. Inami, "Impact: Immersive haptic stylus to enable direct touch and manipulation for surface computing," *Comput. Entertainment*, vol. 8, no. 2, pp. 1–16, 2010.
[16] S. Nagasaka, Y. Uranishi, S. Yoshimoto, M. Imura, and O. Oshiro, "Haptic interface with a stylus for a mobile touch panel," *ITE Trans. Media Technol. Appl.*, vol. 3, no. 4, pp. 279–286, 2015.
[17] J. M. Romano and K. J. Kuchenbecker, "Creating realistic virtual textures from contact acceleration data," *IEEE Trans. Haptics*, vol. 5, no. 2, pp. 109–119, Apr.–Jun. 2012.
[18] H. Culbertson, J. Unwin, and K. J. Kuchenbecker, "Modeling and rendering realistic textures from unconstrained tool-surface interactions," *IEEE Trans. Haptics*, vol. 7, no. 3, pp. 381–393, Jul.–Sep. 2014.
[19] Y. Cho, A. Bianchi, N. Marquardt, and N. Bianchi-Berthouze, "RealPen: Providing realism in handwriting tasks on touch surfaces using auditory-tactile feedback," in *Proc. 29th Annu. Symp. User Interface Softw. Technol.*, 2016, pp. 195–205.

[20] G. Wintergerst, R. Jagodzinski, F. Hemmert, A. Müller, and G. Joost, "Reflective haptics: Enhancing stylus-based interactions on touch screens," in *Proc. Int. Conf. Hum. Haptic Sens. Touch Enabled Comput. Appl.*, Springer, 2010, pp. 360–366.
[21] H. Culbertson and K. J. Kuchenbecker, "Ungrounded haptic augmented reality system for displaying roughness and friction," *IEEE/ASME Trans. Mechatronics*, vol. 22, no. 4, pp. 1839–1849, Aug. 2017.
[22] D. Chen, A. Song, L. Tian, Y. Yu, and L. Zhu, "MH-Pen: A pen-type multi-mode haptic interface for touch screens interaction," *IEEE Trans. Haptics*, vol. 11, no. 4, pp. 555–567, Oct.–Dec. 2018.
[23] Z. F. Quek, S. B. Schorr, I. Nisky, A. M. Okamura, and W. R. Provancher, "Augmentation of stiffness perception with a 1-degree-of-freedom skin stretch device," *IEEE Trans. Human-Mach. Syst.*, vol. 44, no. 6, pp. 731–742, Dec. 2014.
[24] E. Kruijff, S. Biswas, C. Trepkowski, J. Maiero, G. Ghinea, and W. Stuerzlinger, "Multilayer haptic feedback for pen-based tablet interaction," in *Proc. CHI Conf. Hum. Factors Comput. Syst.*, 2019, pp. 1–14.
[25] S. Okamoto, H. Nagano, and Y. Yamada, "Psychophysical dimensions of tactile perception of textures," *IEEE Trans. Haptics*, vol. 6, no. 1, pp. 81–93, First Quarter 2013.
[26] Y. Vardar, C. Wallraven, and K. J. Kuchenbecker, "Fingertip interaction metrics correlate with visual and haptic perception of real surfaces," in *Proc. IEEE World Haptics Conf.*, 2019, pp. 395–400.
[27] H. Culbertson and K. J. Kuchenbecker, "Importance of matching physical friction, hardness, and texture in creating realistic haptic virtual surfaces," *IEEE Trans. Haptics*, vol. 10, no. 1, pp. 63–74, Jan.–Mar. 2017.
[28] R. H. LaMotte, "Softness discrimination with a tool," *J. Neuriophysiol.*, vol. 83, no. 4, pp. 1777–1786, 2000.
[29] R. L. Klatzky and S. J. Lederman, "Tactile roughness perception with a rigid link interposed between skin and surface," *Percep. Psychophys.*, vol. 61, no. 4, pp. 591–607, 1999.
[30] R. L. Klatzky, S. J. Lederman, C. Hamilton, M. Grindley, and R. H. Swendsen, "Feeling textures through a probe: Effects of probe and surface geometry and exploratory factors," *Percep. Psychophys.*, vol. 65, no. 4, pp. 613–631, 2003.
[31] C. Basdogan, F. Giraud, V. Levesque, and S. Choi, "A review of surface haptics: Enabling tactile effects on touch surfaces," *IEEE Trans. Haptics*, vol. 13, no. 3, pp. 450–470, Jul./Sep. 2020.
[32] D. J. Meyer, M. Wiertlewski, M. A. Peshkin, and J. E. Colgate, "Dynamics of ultrasonic and electrostatic friction modulation for rendering texture on haptic surfaces," in *Proc. IEEE Haptics Symp.*, 2014, pp. 63–67.
[33] O. Bau, I. Poupyrev, A. Israr, and C. Harrison, "TeslaTouch: Electrovibration for touch surfaces," in *Proc. 23nd Annu. ACM Symp. User Interface Softw. Technol.*, 2010, pp. 283–292.
[34] G. Ilkhani, M. Aziziaghdam, and E. Samur, "Data-driven texture rendering on an electrostatic tactile display," *Int. J. Hum.–Comput. Interact.*, vol. 33, no. 9, pp. 756–770, 2017.
[35] A. İşleyen, Y. Vardar, and C. Basdogan, "Tactile roughness perception of virtual gratings by electrovibration," *IEEE Trans. Haptics*, vol. 13, no. 3, pp. 562–570, Jul.–Sep. 2020.
[36] T. Fiedler and Y. Vardar, "A novel texture rendering approach for electrostatic displays," in *Proc. Int. Workshop Haptic Audio Interaction Des.*, Mar. 2019. [Online]. Available: https://hal.science/hal-02011782v3/file/Fiedler19-HAID-Electrostatic.pdf
[37] R. F. Friesen, R. L. Klatzky, M. A. Peshkin, and J. E. Colgate, "Building a navigable fine texture design space," *IEEE Trans. Haptics*, vol. 14, no. 4, pp. 897–906, Oct.–Dec. 2021.
[38] H. Kim, J. Kang, K.-D. Kim, K.-M. Lim, and J. Ryu, "Method for providing electrovibration with uniform intensity," *IEEE Trans. haptics*, vol. 8, no. 4, pp. 492–496, Oct.–Dec. 2015.
[39] Y. Vardar, A. İşleyen, M. K. Saleem, and C. Basdogan, "Roughness perception of virtual textures displayed by electrovibration on touch screens," in *Proc. IEEE World Haptics Conf.*, 2017, pp. 263–268.
[40] Y. Vardar, B. Güçlü, and C. Basdogan, "Effect of waveform on tactile perception by electrovibration displayed on touch screens," *IEEE Trans. Haptics*, vol. 10, no. 4, pp. 488–499, Oct.–Dec. 2017.
[41] M. Ayyildiz, M. Scaraggi, O. Sirin, C. Basdogan, and B. N. Persson, "Contact mechanics between the human finger and a touchscreen under electroadhesion," *Proc. Nat. Acad. Sci.*, vol. 115, no. 50, pp. 12668–12673, 2018.
[42] A. Israr, S. Choi, and H. Z. Tan, "Detection threshold and mechanical impedance of the hand in a pen-hold posture," in *Proc. IEEE/RSJ Int. Conf. Intell. Robots Syst.*, 2006, pp. 472–477.
[43] R. M. Friedman, K. D. Hester, B. G. Green, and R. H. LaMotte, "Magnitude estimation of softness," *Exp. Brain Res.*, vol. 191, no. 2, pp. 133–142, 2008.
[44] S. Choi and K. J. Kuchenbecker, "Vibrotactile display: Perception, technology, and applications," *Proc. IEEE*, vol. 101, no. 9, pp. 2093–2104, Sep. 2013.
[45] M. Gabardi, D. Leonardis, M. Solazzi, and A. Frisoli, "Development of a miniaturized thermal module designed for integration in a wearable haptic device," in *Proc. IEEE Haptics Symp.*, 2018, pp. 100–105.
[46] I. Darian-Smith and K. O. Johnson, "Thermal sensibility and thermoreceptors," *J. Invest. Dermatol.*, vol. 69, no. 1, pp. 146–153, 1977.
[47] A. Yamamoto, B. Cros, H. Hashimoto, and T. Higuchi, "Control of thermal tactile display based on prediction of contact temperature," in *Proc. IEEE Int. Conf. Robot. Automat.*, 2004, pp. 1536–1541.
[48] S. Guest et al., "The development and validation of sensory and emotional scales of touch perception," *Attention, Perception, Psychophys.*, vol. 73, no. 2, pp. 531–550, 2011.
[49] E. Baumgartner, C. B. Wiebel, and K. R. Gegenfurtner, "Visual and haptic representations of material properties," *Multisensory Res.*, vol. 26, no. 5, pp. 429–455, 2013.
[50] K. Drewing, C. Weyel, H. Celebi, and D. Kaya, "Systematic relations between affective and sensory material dimensions in touch," *IEEE Trans. Haptics*, vol. 11, no. 4, pp. 611–622, Oct.–Dec. 2018.
[51] I. Hwang, J. Seo, and S. Choi, "Perceptual space of superimposed dual-frequency vibrations in the hands," *PLoS One*, vol. 12, no. 1, 2017, Art. no. e0169570.
[52] G. Park and S. Choi, "Perceptual space of amplitude-modulated vibrotactile stimuli," in *Proc. IEEE World Haptics Conf.*, 2011, pp. 59–64.
[53] S. Mun, H. Lee, and S. Choi, "Perceptual space of regular homogeneous haptic textures rendered using electrovibration," in *Proc. IEEE World Haptics Conf.*, 2019, pp. 7–12.
[54] M. Gabardi, D. Chiaradia, D. Leonardis, M. Solazzi, and A. Frisoli, "A high performance thermal control for simulation of different materials in a fingertip haptic device," in *Proc. Int. Conf. Hum. Haptic Sens. Touch Enabled Comput. Appl.*, 2018, pp. 313–325.
[55] W. M. B. Tiest and A. M. Kappers, "Analysis of haptic perception of materials by multidimensional scaling and physical measurements of roughness and compressibility," *Acta Psychologica*, vol. 121, no. 1, pp. 1–20, 2006.
[56] T. Yoshioka, S. J. Bensmaia, J. C. Craig, and S. S. Hsiao, "Texture perception through direct and indirect touch: An analysis of perceptual space for tactile textures in two modes of exploration," *Somatosensory Motor Res.*, vol. 24, no. 1-2, pp. 53–70, 2007.
[57] B. A. Richardson, Y. Vardar, C. Wallraven, and K. J. Kuchenbecker, "Learning to feel textures: Predicting perceptual similarities from unconstrained finger-surface interactions," *IEEE Trans. Haptics*, vol. 15, no. 4, pp. 705–717, Oct.–Dec. 2022.

Bence L. Kodak received the B.Sc. degree in mechatronics engineering from the Budapest University of Technology and Economics, Budapest, Hungary, in 2019, and the M.Sc. degree in mechanical engineering from the Delft University of Technology, Delft, The Netherlands, in 2022.

He is a Research Engineer with the Delft University of Technology. His current research interests include haptic devices, texture rendering, and human–robot interaction.

Yasemin Vardar received the Ph.D. degree in mechanical engineering from Koç University, Istanbul, Turkey, in 2018.

She is an Assistant Professor with the Delft University of Technology, Delft, The Netherlands. She did her postdoctoral research with the Max Planck Institute (MPI) for Intelligent Systems, Stuttgart, Germany, until 2020. Her research interests include human tactile perception and haptic interfaces.

Dr. Vardar was the recipient of the 2021 NWO VENI Grant, 2018 Eurohaptics Best Ph.D. Thesis Award, IEEE WHC 2017 Best Poster Presentation Award, and TUBITAK Ph.D. Fellowship; she was selected for 2019 MPI Sign Up! Career-building Program. She is currently a co-chair of the Technical Committee on Haptics.